JOURNAL OF MATERIALS SCIENCE **39** (2004) 4199–4210

Comparative creep damage assessments using the various models

H. KAFTELEN, A. BALDAN
Department of Metallurgical and Materials Engineering, University of Mersin, Ciftlikkoy/Mersin, Turkey
E-mail: abaldan@mersin.edu.tr

The creep fracture characteristics of a conventionally cast (CC) MARM-002 superalloy were studied for creep conditions of 1173 K/200–400 MPa using different approaches including the Kachanov-Rabotnov type continuum damage mechanics, grain boundary damage accumulation, and Chen-Argon diffusional cavity growth. A rapid improvement in creep rupture life can be achieved by reducing the Kachanov-Rabotnov damage rate ($\dot{\omega}$) below a critical value of this rate. It is possible that a large improvement in creep resistance would be made by decreasing grain boundary damage rate rather than continuum damage rate since the minimum creep rate ($\dot{\varepsilon}_m$) accelerates rapidly without changing the parameter $\dot{\omega}$.

1. Introduction

The modern nickel-base superalloys such as MAR-M002 are quite complex, and are normally used for cast polycrystalline turbine blades of aircraft jet engines. The microstructure of MAR-M002 alloy consists of the $L1_2$-type ordered γ' [Ni_3(Al, Ti)] phase in a face centered cubic (FCC) solid solution γ-matrix phase, and various types of carbides including MC (where M is metal). The conventional cast (CC) nickel-base superalloys are strengthened through carbide precipitation at the grain boundaries (GB) and γ' precipitation within the grains. The strength of a given alloy is dependent upon such factors as volume fraction, particle size, coarsening rate, and composition of γ' phase. Discrete GB carbides are generally considered beneficial since they reduce GB sliding and therefore improves creep and stress-rupture properties [1]. It was experimentally observed that, to improve the creep ductility, the carbide particle size should be as small as possible; a fine dispersion of carbide particles leads to high creep ductility. It is well accepted that the stress concentrations which can build up around non-deformable second-phase particles during creep deformation may be relieved by two fracture processes: (a) decohesion of the matrix/particle interface or (b) particle cracking. Under high-temperature creep conditions, fracture usually occurs in an intergranular manner by the nucleation, growth and link-up of GB cavities which leads to the crack formation. Therefore, the accumulation of cavities is a dominant life-limiting factor in many superalloys. The modelling of the growth of intergranular cavities during creep has attracted considerable attention in the last 25 years. One of the most critical factors determining the structural integrity of high temperature components is their creep behaviour. During the creep of these superalloys at elevated temperatures a number of micro-mechanistic processes (i.e., γ' coarsening, changing in the grain structure, micro-porosity, formation of cavitation on the GB carbide particles, etc.), which damage the structural integrity of the material [2], operate and are ultimately responsible for failure. The useful life is limited by resistance to this intergranular failure rather than by resistance to deformation although these two processes are interlinked together [3, 4].

Creep rupture in polycrstalline materials at elevated temperatures can occur by a number of different mechanisms. Ashby and Dyson [5] have classified four broad categories of mechanisms: (a) the nucleation and subsequent growth of microscopic cavities, leading to fracture by coalescence, (b) failure by the loss of the cross-sectional area associated with large strains, (c) degradation of the microstructure, by thermal coarsening of particles or by a dislocation-substrature induced acceleration of creep, and (d) finally, environmental degradation. For each mechanism, an equation describing the rate at which damage accumulates, and an associated equation for the rate at which the materials creeps, can be derived [5]. This pair of equations completely describes creep in the material, if that mechanism operates alone and therefore, can be used for life prediction. Therefore, we have used the first three factors in order to analyse the creep fracture characteristics of polycrystalline MARM-002 alloy in the present study.

Better mechanistic understanding of the development of damage in creeping components is essential in the life prediction of parts that have used in service applications. In the last forty years, modeling of damage processes under various creep conditions has been developed to predict the high temperature creep lives of alloys. In order to incorporate the effects of creep damage, Continuum Damage Mechanics (CDM) approach

is applied in which cracks or cavities are equally distributed in all directions. Generally, two different approaches are used to model the creep damage problems identified in the literature [6]: (a) Firstly, there are the purely phenomenological Kachanov-type continuum damage relations, in which a scalar damage parameter ω, which represents the state of the damage, is introduced [7], (b) Secondly, micromechanism-based continuum damage models are used, in which cavitation damage is represented through a dilute distribution of cavitation GB facets. By describing the GB cavities in terms of proper damage variables, CDM has furnished a powerful approach to the creep-damage problems. Kachanov [8] and Rabotnov [9] modeled the creep damage problem through the use of an internal state variable. They introduced a scalar damage parameter ω, which describes the effects of microscopic events phenomenologically and macroscopically, into the creep constitutive equations. With the damage increasing, ω is supposed to vary from $\omega = 0$ for an undamaged material, to $\omega = 1$ for the failed material. This theory of damage therefore, describes the evolution of the phenomena between the virgin state and macroscopic crack initiation. The main problems in this model are connected with neglecting primary creep and formal introduction of the damage parameter. The tertiary creep behavior can simply be modelled using the Kachanov-Rabotnov approach.

The present study aims at investigating the effects of creep damage accumulation on the creep rupture characteristics of the CC MAR-M 002 alloy using the various models such as continuum damage mechanics approach, and different parametric approaches.

2. Material and experimental procedure

In this study, effects of stress and damage accumulation on the basic creep properties of a Ni-based superalloy, MAR-M 002, were investigated using the Kachanov–Rabotnov type continuum damage mechanics approach (CDM), a mechanistic model (i.e., Cocks and Ashby approach) and empirical relationships such as Monkman-Grant and Dobes-Milicka. The bulk composition of this alloy is (in wt%): 2.5 Ta, 10 W, 9.0 Cr, 5.5 Al, 1.5 Ti, 10 Co, 1.5 Hf, 0.05 Zr, 0.14 C, 0.015 B and balance nickel. The creep tests were performed up to failure at a constant temperature (1173 K) by an uniaxial constant-load method. Applied stresses ranging from 200 to 400 MPa were used on specimens with 4-mm gauge diameter. The temperature was kept constant within ± 0.5 K. The creep elongation was recorded continuously using differential transformers. The quantitative evaluations of the cavity size (mean surface area A_c), and cavity density or (number of cavity per cross-section, N_A), and the cavity volume fraction, f_c, were determined using the Cambridge Instrument Q-520 system. For the microstructural evaluations, the scanning electron microscope (SEM) cavity micrographs taken from the entire cross-section of the fractured specimens were used, so that it was ensured that all visible cavities were counted. The linear mean cavity size, c, was evaluated as the square root of the mean caviy particle area (i.e., $A_c^{1/2}$), whereas the intercavity spacing, L, was determined using the following equation $L = 0.5/N_A^{1/2}$.

3. Results and discussion

The phenomenological approaches were used to evaluate the material degradation which accelerates creep rate as a result of cavitation in the tertiary stage. As underlined previously, damage accumulation refers to formation and coalescence of cavities at grain boundaries and the stress-induced changes in the microstructure. From the material's point of view these approaches also involve the determination of cavity growth behavior to predict creep rupture strain as well as creep rupture life of an alloy.

In the present study, the experimental results were analysed to predict the creep rupture life of the alloy using the following approaches: (a) continuum damage mechanics approach, (b) empirical approach, (c) parametric approach, (d) grain boundary damage approach, and (e) diffusional cavity growth approach.

3.1. Continuum damage mechanics approach

It is well known that microdamages usually dominate failure of alloys under various loading conditions. Damage evolution is entirely controlled by the matrix material flow. As mentioned previously, a realistic description of the material's damage behaviour is therefore required. The formalism describing the coupling between damage and deformation, now well known as Continuum Damage Mechanics (CDM) was a seminal concept of Kachanov [8] and later developed by Rabotnov [9]. This approach here has been applied to analyse the creep damage problems in the present alloy.

In physical terms it is simple to consider ω at any instant, as representing the fractional area separated by cracks or cavities which are nearly perpendicular to an applied stress σ_A. As mentioned previously, in the CDM approach, damage is treated as an internal state variable ω for uniaxial stress condition [10]. This approach may be expressed by the following differential equations:

$$\dot{\omega} = \frac{d\omega}{dt} = g(\sigma_A, T, \omega) \tag{1a}$$

$$\dot{\varepsilon} = \frac{d\varepsilon}{dt} = f(\sigma_A, T, \omega) \tag{1b}$$

where both g and f are functions. Equation 1b describes creep rate as a function of the applied stress (σ_A), temperature (T), and current damage level (ω), whereas the evolution of damage is described by Equation 1a [9, 10]. These functions are assumed for the growth of the strain rate with increasing damage and for the rate of growth of the damage parameter, and various constants in these functions are determined so that the description agrees with experimental results. Integration of these equations between appropriate limits, it

is possible to obtained the creep life, strain to failure and shape of a creep curve, for any loading history [11]. The strength of this method is that it allows the progress of damage-accumulation to be followed throughout the life. However, the weaknesses of these functions are practical ones; the data needed to determine the functions f and g in Equation 1 are particularly difficult to obtain [11].

In this approach, material deformation is controlled by the net or effective stress (i.e., the stress calculated over the section which effectively resists the forces, σ_{eff}) according to,

$$\sigma_{\text{eff}} = \frac{\sigma_{\text{A}}}{1-\omega} \tag{2}$$

where ω is defined by $\omega = A_{\text{c}}/D_{\text{s}}$, A_{c} and D_{s} denote the mean cavity particle area and cross section of the specimen, respectively.

Both damage ω and strain ε are assumed to grow with time according to Equation 1. For an uniaxial loading conditions, the creep and damage rates take the following simplest form [5]:

$$\dot{\varepsilon} = A\left(\frac{\sigma_{\text{A}}}{1-\omega}\right)^{\text{n}} \tag{3}$$

$$\dot{\omega} = B\frac{\sigma_{\text{A}}^{\text{m}}}{(1-\omega)^{\mu}} \tag{4}$$

where A, B, n, μ and m are material constants which can be obtained from creep rupture strain data.

Using the Norton's law (power law creep) one can arrive at this expression: $\dot{\varepsilon} = A(\sigma_{\text{eff}})^{\text{n}}$, if we replace the applied stress by the effective stress for damaged material. Assuming $m = \mu$ [12], we can rewrite Equation 4 as follows:

$$\dot{\omega} = \frac{\text{d}\omega}{\text{d}t} = B\left[\frac{\sigma_{\text{A}}}{(1-\omega)}\right]^{\text{m}} \tag{5}$$

In the present study, we defined damage rate (or crack growth rate) by $\dot{\omega} = c/t_{\text{R}}$, where c is the linear mean cavity size, t_{R} is rupture life.

In the CDM approach, the rupture life t_{R}, is given in the following equation [12]:

$$t_{\text{R}} = \frac{1}{B(1+m)\sigma_{\text{A}}^{\text{m}}} \tag{6}$$

In our experimental results we have observed that the amount of the damage (or cavitation) is so small compare to the cross-sectional area of the specimen. Therefore, the effective stress is taken to be equal to applied stress, and that damage rate (crack growth rate) can be expressed as $\dot{\omega} = B\sigma_{\text{A}}^{\text{m}}$. If we substitute this expression into Equation 6 then the rupture life becomes as

$$t_{\text{R}} = \frac{1}{(1+m)\dot{\omega}} \tag{7}$$

Using Equation 5, damage rate $\dot{\omega}$ was plotted against the applied stress σ_{A}, as seen in Fig. 1. Assuming that

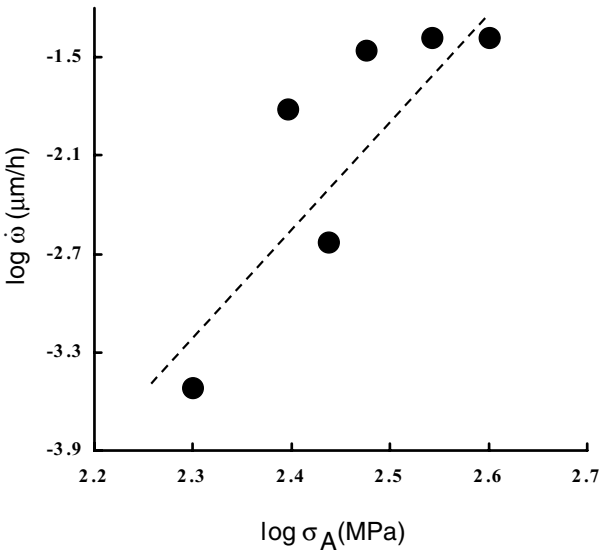

Figure 1 Plotting of Kachanov-Rabotnov type damage rate (or crack growth rate), $\dot{\omega}$, against the applied stress, σ_{A}.

the linear relationship exists in this figure (keeping in mind that there are rather large scatter in the data, and that the curve was best fitted), the value of m, which is the slope of this curve, was determined to be $\sim$7 (i.e., $\dot{\omega} \propto \sigma_{\text{eff}}^{\sim 7}$). In the investigation of the effect of stress deformation on the creep strength of the same alloy [13], the applied stress sensitivity parameter n (i.e., $[\delta \log \dot{\varepsilon}_{\text{m}}/\delta\sigma_{\text{A}}]_{\text{T}}$ was found approximately 8, which is close to that of m value ($\sim$7) in Fig. 1. This implies that power law creep and Kachanov-Rabotnov type damage mechanisms are closely related. Therefore, it would be expected that damage rate $\dot{\omega}$ correlates well with the minimum creep rate $\dot{\varepsilon}_{\text{m}}$, as confirmed in Fig. 2. In Fig. 2, damage rate increases with increasing the minimum creep rate or decreasing creep resistance slowly up to a certain value, and then further increasing the $\dot{\omega}$ parameter rapidly decreases the creep resistance.

As there is an inverse correlation between rupture life and damage rate (crack growth rate) in Equation 7, we plotted the observed rupture life against the observed

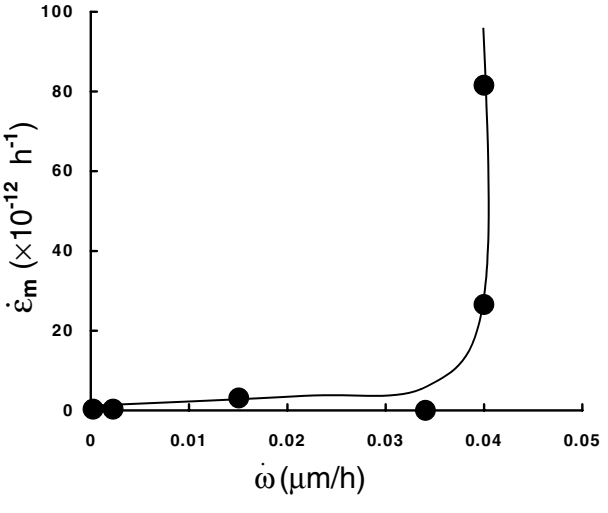

Figure 2 Dependence of minimum creep rate, $\dot{\varepsilon}_{\text{m}}$ on the damage rate, $\dot{\omega}$. Note that creep resistance deteriorated rapidly above a critical value of $\dot{\omega}$.

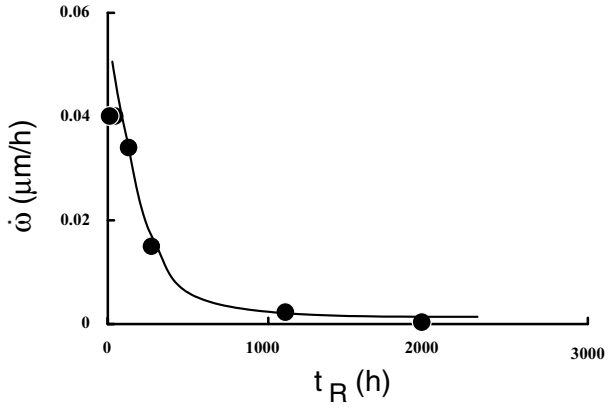

Figure 3 Damage rate $\dot{\omega}$, versus the creep rupture life t_R; rupture life decreases rapidly above a critical value of $\dot{\omega}$.

damage rate $\dot{\omega}$, as shown in Fig. 3. As expected, reducing the damage rate, $\dot{\omega}$ continuously improves the t_R; below a critical value of the damage rate ($\dot{\omega}$) the rupture life extends sharply.

3.2. The empirical approach

As the material is strained, the cavities or cracks grow until they link, leading to an intergranular creep fracture. When the fracture is of this sort, a proportionality [14] is generally found between t_R and $\dot{\varepsilon}_m$. Assuming [14] that creep fracture is controlled by the creep growth of cavities at grain boundaries the result would be consistent with the Monkman-Grant relation. This occurs naturally because the fracture process is linked to the creep process from the very beginning. Many relationships between the secondary or steady state creep rate and the time to rupture have been proposed to analyze data from constant-load accelerated uniaxial creep test. Among these relationships, the best known is the Monkman-Grant relation [15]. In this relationship, the time to fracture in long term creep tensile tests is inversely proportional to power function of the minimum creep rate, for relatively simple alloys such as pure metals and single phase alloys;

$$\dot{\varepsilon}_m^p t_R = C_m \tag{8}$$

where the exponent p is found to range from about ~0.8 to about ~0.95 and the constant C_m ranges from ~2 to ~15, depending on the material and microstructural variables. This constant represent the contribution of secondary creep strain to the total failure strain. Since the exponent p is near unity, Equation 8 becomes as

$$\dot{\varepsilon}_m t_R = C_m \tag{9}$$

Some workers [16] have argued that if continuous nucleation occurs, modelling of the fracture process can lead to a Monkman-Grant relationship (diffusive and plastic coupling of cavity growth and cavity interaction considered). This relationship is the powerful, as well as the simple, method of predicting creep life available, which offers the possibility of long term extrapolation if the same creep deformation mechanism operates during the whole creep life [17]. This relationship can be used to design stress and temperature dependence of operational creep life of high temperature components.

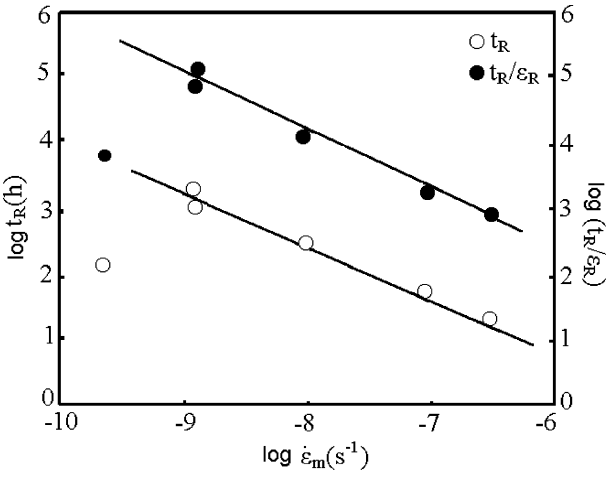

Figure 4 Monkman-Grant and Dobes-Milicka relationships which indicate the similar behavior. ○: t_R (Monkman-Grant); ●: t_R/ε_R (Dobes-Milicka).

A logarithmic plot of time to failure versus minimum creep rate is presented in Fig. 4, indicating that the Monkman-Grant relationship holds. This suggests that the mechanism responsible for the creep failure is controlled by the creep deformation process. An investigation of the CC alloy IN-100 at 900°C/276 MPa creep conditions showed [17] that the reliable life prediction is not possible using this relationship. The differences in behavior of Monkman-Grant relationship for IN-100 and present alloy are due to the differences in the operational deformation mechanism(s). In fact, the deformation mechanism in IN-100 has been predicted to change from Orowan bowing in secondary stage to particle cutting in the tertiary stage [18]. Although creep data were obtained at different stresses, this relationship still exists, suggesting that this correlation is independent of stress, which is consistent with a previous result [19]. In fact, Fig. 5 illustrates near independence of the Monkman-Grant parameter on the stress. For the

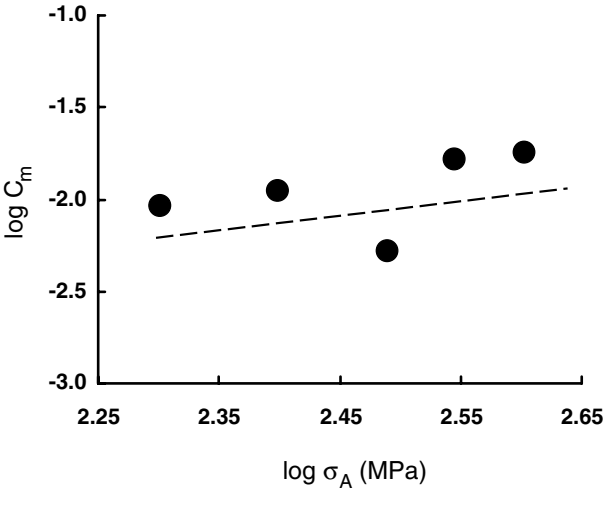

Figure 5 Showing the slow variation of Monkman-Grant ductility C_m with stress, σ_A.

present material, the stress dependence of rupture life and the minimum creep rate were observed [13] to be approximately similar (i.e., $t_R \propto \sigma_A^{\sim -7}$, $\dot{\varepsilon}_m \propto \sigma_A^{\cong 8}$), once again underlines that cavity growth is a deformation controlled process. In the past [20], the combined effects of thin-section size (D) and grain size, d_G on the creep behavior of the CC MAR-M 002 were studied. In this study, it was observed that there was a linear correlation between t_R/d_G and $\dot{\varepsilon}_m/D$ ratios on log-log scales (i.e., a modified Monkman-Grant relationship). The existence of this linear correlation between these ratios was interpreted in terms of the coupling of the grain boundary sliding rate in the secondary creep region with the creep crack growth behavior in the tertiary region. Therefore, we can conclude that the following factors affect the Monkman-Grant relationship: (a) grain size [20], (b) thin-section size [20], and (c) carbide size [17].

For conventional creep tests, it was claimed [21] that an even better correlation of the time to rupture and the minimum creep rate can be obtained using a modified equation in the form:

$$t_R \dot{\varepsilon}_m / \varepsilon_R = C^* \tag{10}$$

where C^* is the appropriate constant. This relationship is depicted in Fig. 4. The validity of this equation has been confirmed on many occasions in the past [i.e., 17, 21]. Although Dobes-Milicka relationship was originally proposed to overcome the scatter problems associated with the Monkman-Grant expression for creep life prediction [17, 21], both relationships are quite similar in the present work, indicating that the scatter did not reduce in Fig. 4. This result illustrates that both relationships can be equally used to describe the rupture behavior for this alloy. As is the case for the Monkman-Grant expression, Dobes-Milicka relationship may also be consistent with the model based on prediction of intergranular creep fracture when cavities grow coupled by power law creep with GB diffusion mechanism [22].

Nix *et al.* [14] have investigated the Monkman-Grant relationship theoretically by assuming that cavity growth occurs by plastic flow at the tip of a GB crack by power law creep. They also assumed that the cavities lie along grain boundaries and grow plastically in response to the applied stress as modified by wedge cracks. The growth rates of wedge type cracks by GB sliding mechanism would depend on the stress dependence of the matrix strain rate and observed stress sensitivity of rupture life. Their main prediction is that the Monkman-Grant constant depends on microstructure through the spacing between cavities, grain size, and only weakly on the initial cavity size. Provided that all other terms in Equation 15 in [14] were held constant, Nix *et al.*'s equation can be written as

$$t_R \propto \frac{\sigma_A^{n/(n+2)} L^{(n-2)/(n+2)}}{\dot{\varepsilon}_m} = A' \tag{11}$$

Note that logarithmic term in this equation was ignored. This relationship predicts that the creep rupture life is proportional to applied stress (σ_A), intercavity spacing

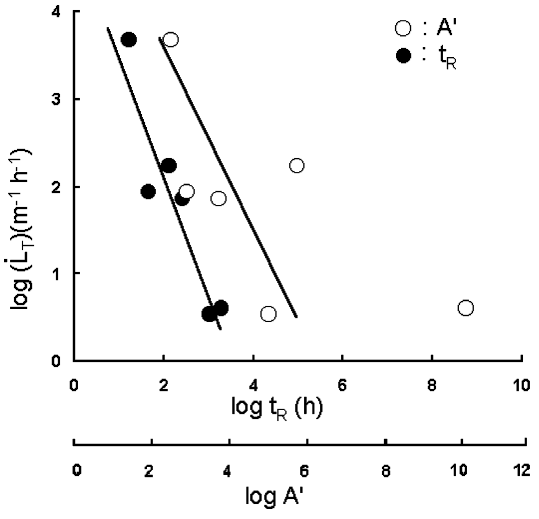

Figure 6 The effect of grain boundary damage rate accumulation, $\dot{L}_T$, on A' parameter, and observed rupture life, t_R. ○: A' (Nix *et al.* model); ●: t_R (observed).

(L), and minimum creep rate ($\dot{\varepsilon}_m$). According to this model the Monkman-Grant ductility should depend on applied stress which is nearly consistent with present observation (see Fig. 5).

In the present work, to explain the effects of applied stress, intercavity spacing, and minimum creep rate on the GB damage rate, this theoretical model was used. In order to evaluate the effect of damage accumulation on the rupture characteristics damage rate accumulation ($\dot{L}_T$) was defined below (see Equation 14). Using the power law creep exponent n approximately equal to 8 for the present alloy observed previously [13], the right-hand side of Equation 11 (i.e., A' parameter) was plotted against the GB damage rate accumulation ($\dot{L}_T$), on log-log scale, as presented in Fig. 6; there is an inverse linear relationship between calculated parameter A' and $\dot{L}_T$.

Since the cavity nucleation is a key step in creep fracture, some improvements in creep rupture life can be achieved by reducing the cavity nucleation or, equivalently, by increasing the mean cavity spacing between the microcracks (see Equation 11). Therefore, an improvement in creep life in MAR-M 002 can be made by decreasing damage rate accumulation ($\dot{L}_T$) (see Fig. 6), which can be obtained by inhibiting cavity nucleation between carbide-matrix interfaces [23]. Some theories of intergranular creep fracture assume that cavity voids, nucleating on grain boundaries, grow by stress-induced diffusion. All diffusion controlled models for creep rupture therefore result in a relatively small dependence of the rupture time on the applied stress [24]. On the other hand, Nix *et al.*'s equation predicts that rupture life is expected to be more sensitive to applied stress [24] than that indicated by diffusional cavity growth models (models for stress-induced diffusion lead to conclusion that t_R should vary as $1/\sigma_A$ [25] or perhaps as $1/\sigma_A^3$ [26]). This can be contrasted to the typical Monkman-Grant phenomenology (Equation 9). That is, the Monkman-Grant relationship suggests that the cavity growth rate should be proportional to the stress to higher power values rather than 1–3 for purely diffusional cavity growths. Using the observed

power exponent of the present alloy [13] (i.e., $\dot{\varepsilon}_m = A\sigma_A^{\cong 8}$), the stress exponent of t_R was found to be approximately (−7) in Nix *et al*. model (Equation 11), which is consistent with the previous experimental result, i.e., $t_R \propto \sigma_A^{-7}$ [13]. Therefore, on the basis of high power stress dependency of t_R in the present work, it is suggested that cavity growth is not controlled effectively by the stress driven diffusion. In fact, in a previous report [2], the coupled power law creep with GB diffusion cavity growth mechanism was predicted to operate in the tertiary creep regions in the present alloy.

3.3. The parametric approach

The amount of damage developed during the creep process significantly affects the strain attainable. The rupture strain should be interpreted as the strain to extend a crack distribution including a crack of critical size which leads to failure. As shown in Fig. 7, there is a complicated relationship between the rupture strain (ε_R) and the cavity volume fraction (f_c). Dependence of the creep rupture strain on the cavity density (N_A) was also constructed in Fig. 8, which is similar to the curve in Fig. 7. It was observed previously that there was an almost linear correlation between the cavity and carbide particle densities in the present alloy [23]. Assuming the cavities occurred on the carbide particles which is based on the fact that there is one-to-one correlation between carbide particle and cavity densities [27], it is therefore concluded that the variation of rupture strain in Fig. 7 would be due to the variation of the carbide particle densities along grain boundaries. As observed previously [3], the nucleation stress to produce critical size for failure becomes higher as the carbide particle density increases. It is therefore possible that the maximum in rupture strain in Fig. 7 is due to the critical sized-cavities which cease cavity nucleation because no further carbides are left to cavitate. In an investigation on intergranular cavitation in a superalloy, the largest

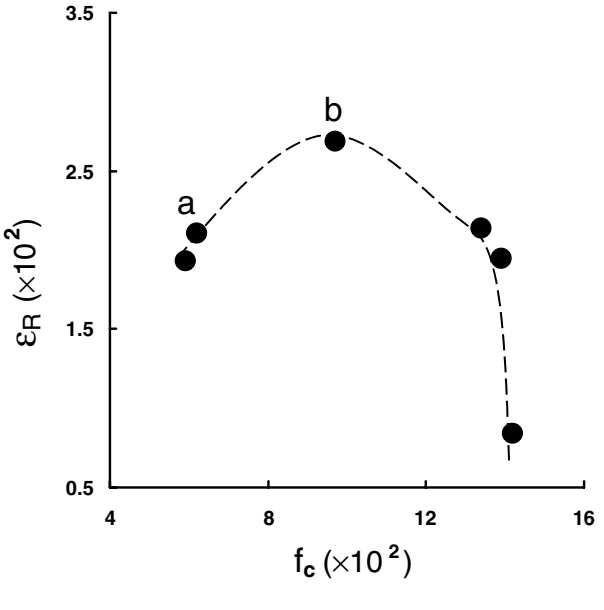

Figure 7 Showing the complicated relationship between the cavity volume fraction, f_c, and the rupture ductility, ε_R.

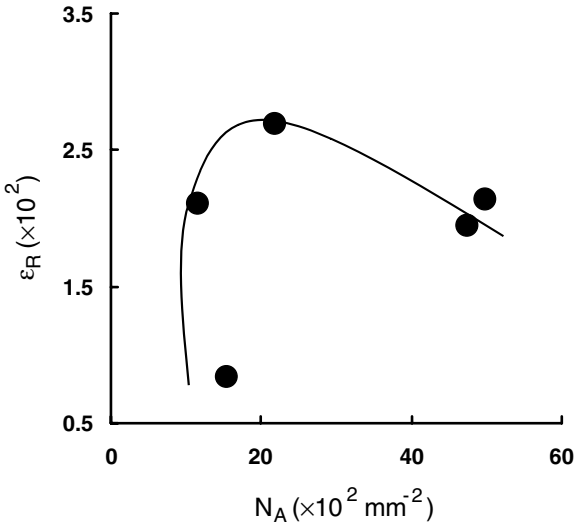

Figure 8 There is an increase and decrease in ductility with increasing cavity density (N_A).

creep strain was also observed where the boundaries saturate with cavities [28], which is consistent with the present result.

It is generally believed that cavities are nucleated at geometrical irregularities or second phase particles, such as carbide particles, on the grain boundaries where high stress concentration can develop. Cavity formation occurs either by particle fracture or by seperation (or decohesion) of the particle-matrix interface. Typical cavity morphologies (shapes, sizes, locations) produced after failure are shown in Fig. 9. From these micrographs we can classify the cavities as two types of decohesion (i.e., cavities originating between carbide-matrix interface): (a) the cavities occurring as partially debonded cavities along the grain boundaries, as seen in Fig. 9a, which corresponds to the point a in Fig. 7, and (b) the second type occurs as fully debonded cavities (or decohesion) (see Fig. 9b), which corresponds to the highest strain observed (the point b) in Fig. 7. The observation of partially- and fully-debonded interfaces at different strains suggests that the cavitation process is strain-controlled. It is expected that particles which are roughly equiaxed will generally suffer interfacial decohesion after certain amount of plastic strain, while irregularly shaped particles with large aspect ratios often fail by internal fracture. Generally, smaller carbide particles have a smaller constrained zone than large particles, so larger particles would require more strain to produce complete debonding, as in the case of Fig. 9b. Therefore, it is likely that decohesion at the carbide-matrix interface evolves progressively with strain.

The complicated relation in ε_R versus f_c plot (Fig. 7) underlines the fact that parameters other than the cavity volume fraction, f_c, are important in determining creep rupture strain. For a number of materials (see e.g., [29]), it has been found empirically that the volume fraction of cavities f_c, can be related to the strain (ε_R), rupture time (t_R) and the applied stress (σ_A) at a given temperature:

$$f_c \propto \varepsilon_R t_R \sigma_A^q \qquad (12)$$

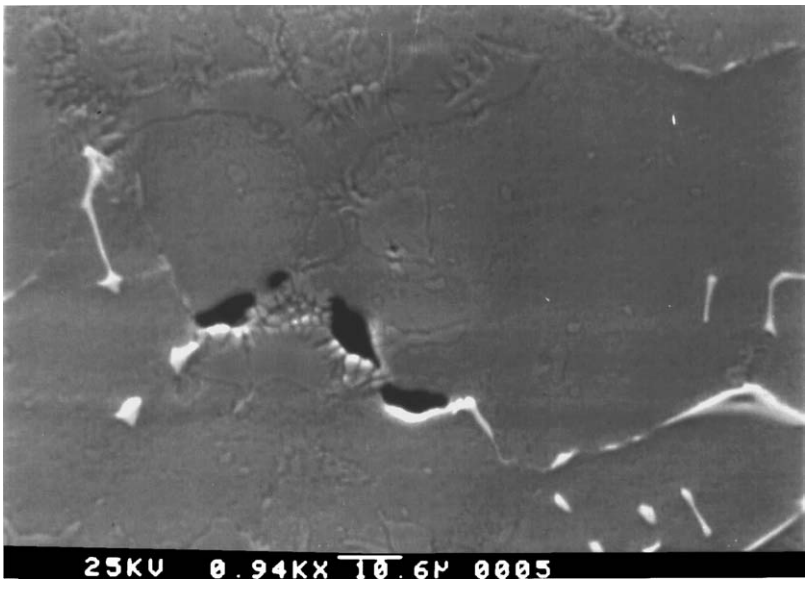

(a)

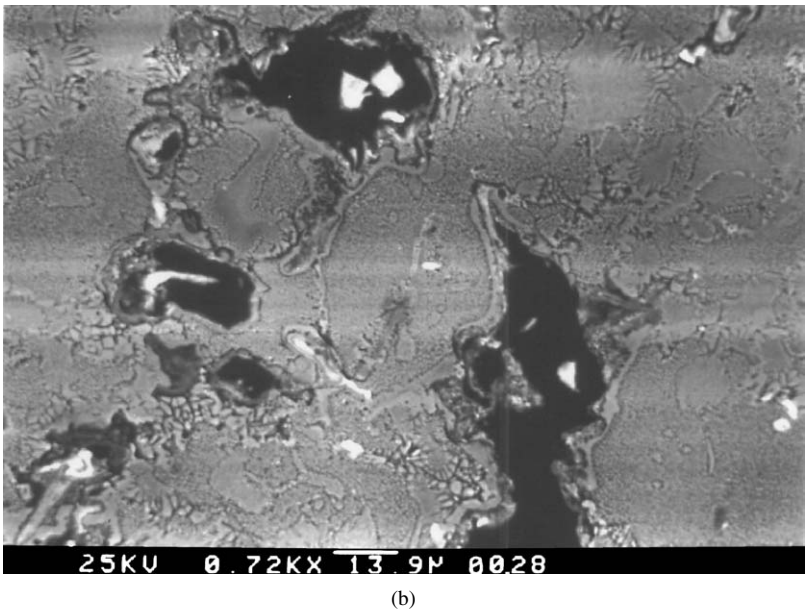

(b)

Figure 9 Two types of decohesion morphologies observed after fracture: (a) the partial decohesion corresponding to point a in Fig. 7 and (b) fully-decohesion between carbide particle-matrix interfaces representing the point b in Fig. 7.

where q is constant. In the present study, this parametric approach has been correlated using the value of $q = 2$. As Fig. 10 gives an approximately linear correlation between f_c and the $\varepsilon_R t_R \sigma_A^2$ product; it is then possible that the nucleation of cavity appeared to start right after loading and proceeded steadily through all creep stages, and that it is the cavity growth process which dominantly affected creep rupture life since this linear curve starts approximately at the origin. Using Fig. 10, it is possible to predict the rupture life, although there is a large scatter at a data. In the past some workers (i.e., [4, 29]) have tried to correlate the cavity volume fraction and the $\varepsilon_R t_R \sigma_A^q$ product for a number of engineering alloys and single-phase materials. Woodford [29] has found that such a linear correlation also existed in pure nickel (i.e., the stress exponent q was 7.5 for pure nickel). This difference in the q value between pure nickel and a commercial nickel-base alloy such as

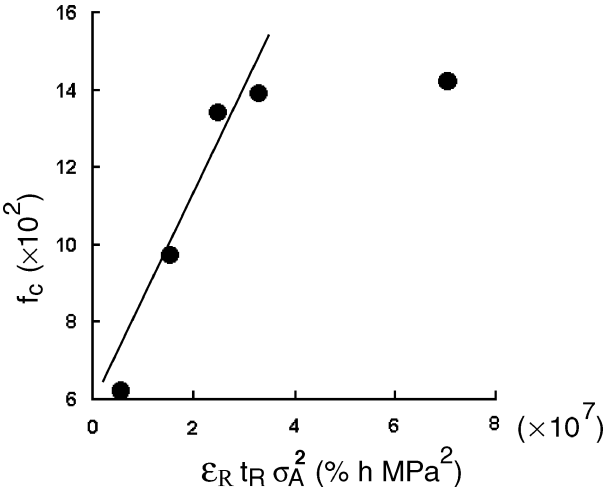

Figure 10 Correlation between cavity volume fraction f_c and the $\varepsilon_R t_R \sigma_A^2$ product at a constant temperature (1173 K).

MAR-M 002 is not unexpected as the microstructural factors, which would influence creep and cavitation, would be different for two materials.

3.4. Grain boundary damage approach

At elevated temperatures, GB cavitation is a general phenomenon accompanying the process of creep rupture: cavity nucleation at the grain interfaces grow to coalesce with each other until the remaining ligament can no longer support the sustained loads, and as a result, premature failure takes place. As emphasized previously, intergranular creep fracture can occur through the development of closely spaced cavities on grain boundaries oriented normal to the applied stress. The growth of intergranular cavities under creep conditions is of considerable technological interest. The intergranular nature of creep fracture indicates that the most damaging cavities are those which exist at grain boundaries. The increase in the strain rate is assumed to occur as a result of growth and accumulation of cavities along grain boundaries [4]. Prediction of creep rupture life is thus important for the design of structural components subjected to elevated temperatures. In the present work, a parameter was defined as a total length of damaged grain boundary (or GB damage accumulation), $L_T(m^{-1})$, in order to investigate the effect of damage accumulation on the rupture life:

$$L_T = N_A \times c \tag{13}$$

and also the GB damage rate accumulation $\dot{L}_T(m^{-1}\ h^{-1})$ is defined as

$$\dot{L}_T = \frac{L_T}{t_R} \tag{14}$$

To show the extent of damage rate on the observed creep rupture life, t_R was plotted against $\dot{L}_T$ on log-log scales, as seen in Fig. 6, indicating that decreasing damage rate continuously improves the creep rupture life, which is consistent with a previous work [30]. In a previous study [13] it was observed that there was a linear correlation between the damage rate and the stress. Therefore, increasing the applied stress increases the damage rate, in turn it causes rupture life to deteriorate. The $\dot{L}_T$ versus t_R plot gives better correlation comparing with $\dot{L}_T$ versus A' plot (see Fig. 6), which is probably due to the fact that grain size was assumed to be independent of predicted rupture life A'. In addition, the similarity between two curves in Fig. 6 suggests that the variation of the observed rupture life is effectively controlled by the applied stress, intercavity spacing and the minimum creep rate.

Creep lifetime in high temperature alloys is controlled by the evolution with time of either mechanical or microstructural instabilities which manifest themselves as the tertiary stage of creep. The creep damage tolerance parameter λ, defined by $\lambda = \varepsilon_R/(\dot{\varepsilon}_m \times t_R)$, originally proposed by Leckie and Hayhurst [10], which gives an information regarding to the damage mechanism(s) operating during creep, might be used to identify the dominant creep damage mechanism(s) responsible for the tertiary creep. For this purpose they constructed a "diagnostic" diagram on the basis of ε_R versus $\dot{\varepsilon}_m t_R$. Therefore, according to their calculations, rupture failure dominated by GB cavitation tends to occur in the range $2.5 > \lambda > 1$, and failure dominated by microstructure degradation (such as γ' coarsening, formation of cavities or voids) occurs at values of λ around 10 or higher. In the present work, the parameter λ was calculated to be between ~1.2 and ~2.1. This observation suggests that the possible source of effective creep damage is the development of GB cavities, which is consistent with the cavitation observed (see Fig. 14 below).

Cocks and Ashby [11] have developed approximate analytical equation in order to define creep damage rate, which is called mechanistic model, under uniaxial stress state condition by power law creep:

$$\frac{df_c}{dt} = \dot{\varepsilon}_0 \left(\frac{\sigma_1}{\sigma_0}\right)^n \left[\frac{1}{(1-f_c)^n} - (1-f_c)\right] \tag{15}$$

where f_c is the cavity volume fraction, df_c/dt is damage rate, $\dot{\varepsilon}_0$ (s^{-1}) is the creep constant, σ_0 is the mean stress in damaged region when cavities are heterogeneously distributed, σ_1 is the principal stress, and n is the power law creep exponent. They theoretically compared their model (i.e., the creep deformation model based on power law creep) with Kachanov-Rabotnov continuum damage model. They concluded that the mechanistic equation has a close resemblance to that of continuum damage mechanics when cavity volume fraction has a large value (since the $[-(1-f_c)]$ term is neglected). However, when f_c or ω approaches to zero (as it is the case for most of the life) there are important differences between these mechanisms. Physically the continuum model states that the damage rate is finite even when there is no damage (f_c or $\omega = 0$), whereas the mechanistic model states that the damage rate is zero under these conditions, although Equation 5 yields not zero value but very low values for primary and secondary creep.

Existence of the large damage in an alloy leads to a similarity between Equations 5 and 15 (i.e., $m = n$ and $B = \dot{\varepsilon}_0/\sigma_0^n$). To calculate the mechanistic damage rate (df_c/dt) using Equation 15, the following constants were used for various applied stresses ($\sigma_A = 200$–400 MPa) and observed cavity parameters f_c : $\sigma_0 = 4097 \times 10^6\ Nm^{-2}$ [31], $\dot{\varepsilon}_0 = 2{,}627 \times 10^{-10}\ s^{-1}$ [31], and for polycrystalline materials, σ_1 may be taken to be equal to $\sigma_A/2$. Fig. 11 shows the relationship between mechanistic damage rate and GB damage rate accumulation. Assuming a linear correlation exits in this figure then we can conclude that there is one-to-one correspondence between two parameters (i.e., $\dot{L}_T \propto (df_c/dt)^{\approx 1}$).

However, Fig. 12 shows the variation of the Kachanov-Rabotnov type damage rate ($\dot{\omega}$) against GB damage rate accumulation ($\dot{L}_T$), which indicates that first increasing the $\dot{L}_T$ continuously increases the $\dot{\omega}$ parameter, up to a certain value, and that above this value $\dot{\omega}$ saturates further increasing $\dot{L}_T$, which is consistent with the previous findings [32, 33]. This saturation behavior

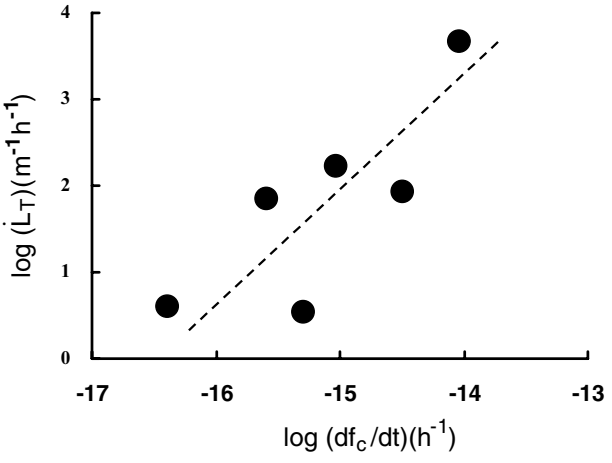

Figure 11 Relationship between grain boundary damage rate accumulation ($\dot{L}_T$) and mechanistic damage rate (df_c/dt), calculated using the Cocks and Ashby model (Equation 15).

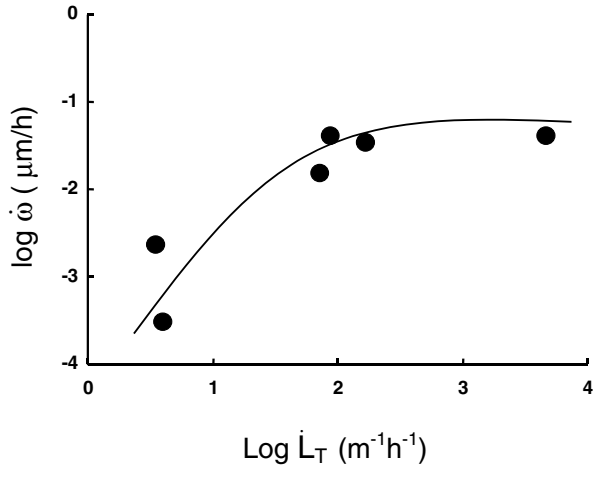

Figure 12 Continuum damage rate, $\dot{\omega}$, versus the grain boundary damage rate, $\dot{L}_T$.

occurs because parts of the grain boundaries are completely cavitated and the microcrack length on these grain boundaries ceases to increase [32]. However, this important feature has never been predicted by the conventional creep-damage theory. As Fig. 12 confirms experimentally the mechanistic approach is closely related to the CDM since there is one-to-one correspondence between the GB damage accumulation approach and the mechanistic approach (see Fig. 11). Based on the mechanistic approach [11] and the present observation, it is suggested that the mechanistic and continuum damage models show a similar behavior up to a certain value of $\dot{L}_T$ (see Fig. 12). Above the critical value of $\dot{L}_T$, continuum damage-rate $\dot{\omega}$, reaches to a limiting value, which appears consistent with the Cocks and Ashby's work [11]. From Figs 2 and 12, it is possible to conclude that minimum creep rate should be proportional to GB damage rate accumulation, $\dot{L}_T$. In fact, such a linear correlation was observed in a previous study [13]. According to Fig. 2, it is proposed that above the critical value of $\dot{\omega}$ the minimum creep rate would be expected to be controlled by mechanistic damage rate, df_c/dt, or GB damage rate accumulation, rather than continuum damage rate, $\dot{\omega}$, since the minimum creep rate accelerates rapidly without changing the parameter $\dot{\omega}$. Therefore, from Fig. 12, it is concluded that GB damage approach better describes the creep damage process rather than the continuum damage model. In supporting this, when the material is in the virgin state the damage rate reaches a finite value, which indicates the inherent weakness of the CDM approach.

3.5. Diffusional cavity growth approach

The cavity growth at elevated temperatures is generally thought to be controlled by surface and GB self-diffusion, although other possible mechanisms such as GB sliding, dislocation slip, etc., may be operational as well. Two types of diffusive growth mechanisms can be distinguished on the basis of controlling diffusion process: (a) cavity growth controlled by GB diffusion (equilibrium growth) [25], and (b) cavity growth controlled by surface diffusion (non-equilibrium growth) [26]. Chen and Argon [34] have developed a theoretical model for cavity growth mechanism based on a diffusional growth of GB cavities of both quasi-equilibrium shape and non-equilibrium shape in the presence of power law creep. An equilibrium shape of cavities (or round shape) occurs along the GBs when surface diffusion is rapid enough. However, GB cracks initiate as round type cavities (like in Fig. 14a) propagated by the growth of the cavities under the joint action of vacancy diffusion and GB sliding and link up to form a continuous crack (as seen in Fig. 14b). Therefore, conditions do not always allow this quasi-equilibrium cavity shape, and GB cavities sometimes have an elongated, or crack-like shape. In general, a crack-like cavity grows under an interaction between GB diffusion and power-law creep [34].

The influence of creep flow (power-law creep) on cavity is known to be important in many circumstances. The interaction of GB diffusion and dislocation creep of the grains around a single cavity has been studied numerically by Needleman and Rice [31] for a material subject to uniaxial tension remote from the cavity. The coupling between diffusion and power law creep can be expressed in terms of stress and temperature dependent "material length scale" or a characteristic diffusion

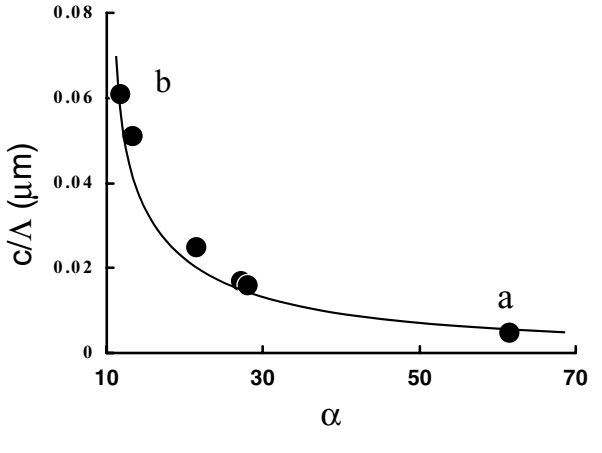

Figure 13 Inverse corelation between the normalized cavity size c/Λ and the coupling or (transition) parameter α; a transition from a quasi-equilibrium mode to a crack-like mode occurs through the point a to the point b.

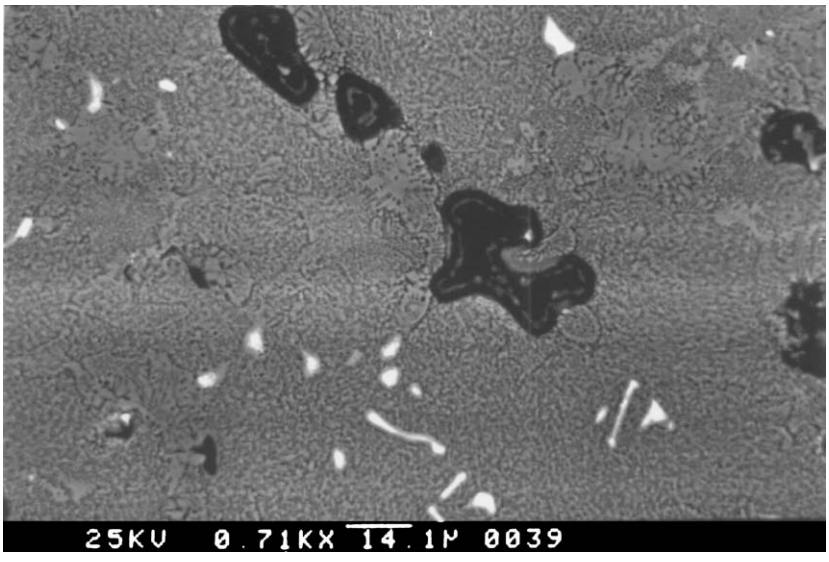

(a)

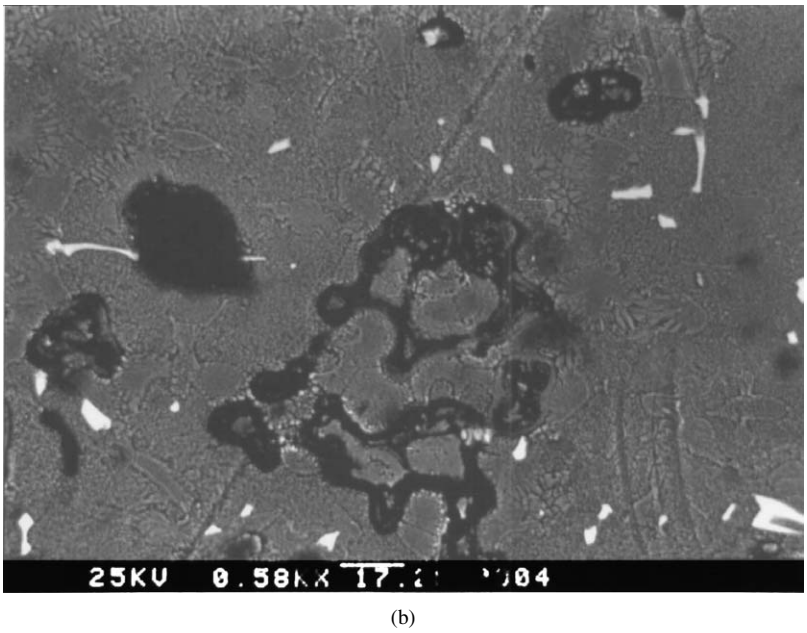

(b)

Figure 14 Cavity morphologies observed after fracture at various creep conditions: (a) the round shape cavity morphology along the grain boundaries, which corresponds to the point **a** in Fig. 13 and (b) the irregular type cavity morphology in the vicinity of eutectic ($\gamma + \gamma'$) pools, which corresponds to the point **b** in Fig. 13.

distance as follows [31]

$$\Lambda = [D_B \delta_B \Omega \sigma_\infty / (kT\dot{\varepsilon}_\infty)]^{1/3} \tag{16}$$

where D_B ($m^2 s^{-1}$) is the GB diffusion rate constant, δ_B(m) the GB width, Ω (m^3) the atomic volume, σ_∞ (σ_A) the applied stress, $\dot{\varepsilon}_\infty$ the associated creep strain rate (or the minimum creep rate $\dot{\varepsilon}_m$), k Boltzmann's constant (equal to 1.38×10^{-23} J K^{-1}), and T the absolute temperature. Note that $\delta_B D_B$ was calculated using the Arrhenius-type equation. The characteristic diffusion distance is a function of material properties, temperature and applied stress; Λ decreases with increasing temperature and stress. In the present study, the diffusional cavity growth mechanism was considered to control the damage accumulation process involving the cavity nucleation and growth. A coupling (or transition) parameter α between quasi-equilibrium and non-equilibrium shape of cavities can be defined [34] as

$$\alpha = 2\left\{\left(\frac{\Lambda}{c}\right)\left[\ln\left(1+\frac{\Lambda}{c}\right) + \frac{1}{(1+\Lambda/c)^2} \times \left(1 - \frac{1}{4(1+\Lambda/c)^2}\right) - \frac{3}{4}\right]\right\}^{1/2} \tag{17}$$

which is the ratio of effective boundary diffusional conductance to surface diffusional conductance. The ratio of cavity size to diffusion distance c/Λ, which is also called normalized cavity size, affects the transition from the quasi-equilibrium mode to the crack-like mode. Using the various material constants for MAR-M 002 [11] the characteristic diffusion distance (or length) (Λ) and the coupling parameter (α) were calculated for various σ_A (or σ_∞) and $\dot{\varepsilon}_{min}$ ($\dot{\varepsilon}_\infty$) values.

As shown in Fig. 13, the normalized cavity size (c/Λ) was plotted against the transition (or coupling) parameter (α) indicating that the decreasing the transition parameter α leads to an increase of the normalized

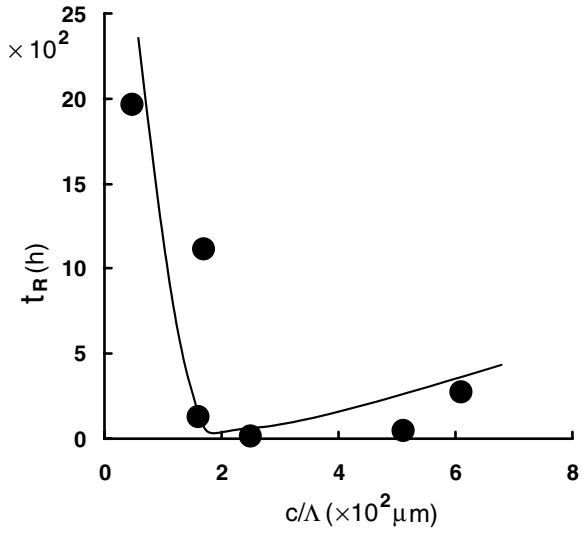

Figure 15 Dependence of creep rupture life t_R on normalized cavity size c/Λ. Note that the rupture life improves rapidly below a critical value of the normalized cavity size.

cavity size. Typical cavity morphologies observed during the transition from quasi-equilibrium to crack-like shape are presented in Fig. 14. Fig. 14a gives a cavity morphology existing as round type cavities along the GBs representing the point (a) in Fig. 13, whereas irregular shape of cavities exist in Fig. 14b which corresponds to point b in Fig. 13; note that the irregular shapes of cavities suggest that they were formed by the agglomeration of individual cavities. From the inspection of these cavities observed at different creep conditions, it is suggested that the tendency from quasi-equilibrium mode to crack-like mode occurs as normalized cavity size decreases (i.e., change from quasi-equilibrium mode to crack-like mode through point a to point b in Fig. 13), as expected. Dependence of rupture life t_R on the normalized cavity size c/Λ was also plotted in Fig. 15; the creep rupture life extends rapidly as the c/Λ value decreases below a critical value where cavity shape changes from the crack-like (see Fig. 14b) to the quasi-equilibrium (see Fig. 14a). Therefore, it is concluded that there is a tendency from quasi-equilibrium to crack-like shape as the cavity size decreases or the characteristic diffusion distance increases, which in turn improves the rupture life. The question now arises why the rupture life deteriorates drastically above the critical value of c/Λ. It is possible that occurrence of the lowest creep rupture life ($\sim$17 h) in Fig. 15 has occurred due to the simultaneous effects of creep (i.e., coupled GB diffusion and power law creep) and non-equilibrium cavity shape (i.e., crack-like mode); as mentioned previously it was shown [2] that the cavity growth was controlled by coupled power law creep and GB diffusion in the tertiary creep region for the same alloy, which is consistent with the present finding.

4. Conclusions

In the present work, the effect of cavitation on the creep fracture characteristics of CC MAR-M 002 alloy was investigated at the creep conditions of 1173 K/200–400 MPa using the various approaches such as continuum damage and GB damage approaches. It was observed that the creep rupture life (t_R) can be improved continuously by decreasing the continuum damage rate ($\dot{\omega}$) below its critical value. A large improvement in the creep rupture life can also be made by reducing the normalised cavity size (c/Λ) below a critical value; it was suggested that non-equilibrium cavity (i.e., crack-like cavity) with coupled creep damage mechanism occurs where the lowest creep rupture life ($\sim$17 h) exits. The complicated relationship between cavity volume fraction (f_c) and rupture strain underlines the fact that there are other parameters which control the rupture strain. In fact, an approximate linear correlation was observed between the cavity volume fraction and the rupture strain ε_R, stress, σ_A, rupture life, t_R, through the $\varepsilon_R t_R \sigma_A^2$ product. Therefore, it is possible that this linear correlation can be used for predicting the creep rupture life.

The minimum creep rate ($\dot{\varepsilon}_m$) decreases with increasing the damage rate ($\dot{\omega}$) slowly up to a certain value; as the damage rate reaches a finite value above this critical value it is suggested that appreciable improvement in creep resistance can be achieved by reducing the GB damage rate accumulation ($\dot{L}_T$) rather than continuum damage rate ($\dot{\omega}$). From the comparison of continuum and GB damage rate it is possible that the GB damage accumulation model is more convenient than continuum damage model for the prediction of cavity growth because the $\dot{\omega}$ parameter keeps constant above the critical value of $\dot{L}_T$.

References

1. A. BALDAN, *J. Mater. Sci.* **26** (1991) 3409.
2. *Idem., ibid.* **33** (1998) 3629.
3. *Idem., Z. Metallkd.* **83** (1992) 10.
4. *Idem., Phys. Status. Solidi(a)* **128** (1991) 383.
5. M. F. ASHBY and B. F. DYSON, *Proc. ICF6* **3** (1984).
6. P. ONCK and E. VAN DER GIESSEN, *Mech. Phys. Solids* **47** (1999) 99.
7. D. R. HAYHURST, P. R. BROWN and C. J. MORRISON, *Philos. Trans. R. Soc. London Ser.* A **311** (1984) 131.
8. L. M. KACHANOV, *Izv. Akad. Nauk.USSR Otd. Tekh. Nauk* **8** (1958) 26.
9. YU. N. RABOTNOV, "Creep Problems in Structural Members" (North Holland, Amsterdam, 1969).
10. F. A. LECKIE and D. R. HAYHURST, *Acta Metall.* **25** (1977) 1059.
11. A. C. F. COCKS and M. F. ASHBY, *Progr. Mater. Sci.* **27** (1982) 189.
12. J. BETTEN, *Arch. Appl. Mec.* **71** (2001) 78.
13. A. BALDAN, *J. Mater. Sci. Lett.* **17** (1998) 1549.
14. W. D. NIX, D. K. MATLOCK and R.J. DIMELFI, *Acta Metall.* **25** (1977) 495.
15. F. C. MONKMAN and N. J. GRANT, *Proc. ASTM* **56** (1956) 593.
16. K. DAVANAS and A. A. SOLOMON, *Acta Metall.* **38** (1990) 1905.
17. A. BALDAN, *J. Mater. Sci. Lett.* **11** (1992) 1315.
18. *Idem., Z. Metallkd.* **83** (1992) 5.
19. G. H. EDWARD and M. F. ASHBY, *Acta Metall.* **27** (1979) 1505.
20. A. BALDAN, *Mater. Sci. Tech.* **13** (1997) 1033.
21. F. DOBES and K. MILICKA, *Met. Sci.* **10** (1976) 382.
22. J. CADEK, "Creep in Metallic Materials" (Elsevier, Amsterdam, 1988) p. 339.
23. A. BALDAN, *Z. Metallkd.* **85** (1994) 6.

24. D. K. MATLOCK and W. D. NIX, *J. Nucl. Mater.* **56** (1975) 145.
25. D. HULL and D. E. RIMMER, *Phil. Mag.* **4** (1959) 673.
26. T. J. CHUANG and H.R. RICE, *Acta Metall.* **21** (1973) 1625.
27. A. BALDAN, *J. Mater. Sci. Lett.* **16** (1997) 780.
28. M. A. CAPANO, A. S. ARGON and I.-W. CHEN, *Acta Metall.* **37** (1989) 12.
29. D. A. WOODFORD, *Met. Sci. J.* **3** (1969) 234.
30. R. G. FLECK, C. J. BEEVERS and D. M. R. TAPLIN, *Metal. Sci.* (1976) 413.
31. A. NEEDLEMAN and J. R. RICE, *Acta Met.* **28** (1980) 1315.
32. Y. LIU, Y. KAGEYAMA and S. MURAKAMI, *Int. J. Mech. Sci.* **40** (1998) 147.
33. K. KIKUCHI and Y. KAJI, *J. Soc. Mater. Sci. Japan* **44** (1995) 1244.
34. I.-W. CHEN and A.S. ARGON, *Acta Metall.* **29** (1981) 1759.

Received 15 July 2003
and accepted 5 March 2004